Roll-to-Roll Production of Catalyst Coated Membranes for Low-Temperature Electrolyzers

*Janghoon Park, Zhenye Kang, Guido Bender, Michael Ulsh, Scott A. Mauger**

Chemistry and Nanoscience Center, National Renewable Energy Laboratory, 15013 Denver West Parkway, Golden, CO 80401, United States

* Corresponding author. Email address: scott.mauger@nrel.gov (S. A. Mauger)

ABSTRACT: This work demonstrates a roll-to-roll (R2R) process for direct coating of anode catalyst layers on a polymer electrolyte membrane for low-temperature water electrolysis. To develop this process, catalyst ink formulation, ink-membrane interactions, and coating quality were studied. The catalyst inks were a mixture of iridium oxide (IrO_2) and Nafion in a water and alcohol dispersion medium. The type of alcohol (methanol, ethanol, propanols) and water-to-alcohol ratio were varied to determine their influence on membrane swelling, dispersion quality, and coatability. Small-scale coating samples were prepared to understand coating uniformity and formation of irregularities. Subsequently, two water/1-propanol ratios (90:10 and 75:25) were down-selected for R2R slot-die coating. The R2R catalyst-coated membrane (CCM) coating process increased catalyst layer production throughput by over 500x compared to our standard lab-scale spray coating. The CCMs obtained from this process were tested as single-cell membrane electrode assemblies. They exhibited a cell voltage of

1.91 V at a current density of 2 A/cm^2, which is comparable to spray-coated CCMs. In conclusion, the work presented here demonstrates a continuous, scalable manufacturing process that eliminates the need for the decal transfer step typically used in CCM production.

Keywords: *Polymer electrolyte membrane water electrolyzers, roll-to-roll, slot-die coating, catalyst coated membranes, iridium oxide, catalyst inks*

1. Introduction

Low temperature electrolysis (LTE) is increasing in interest due to its potential to produce low-cost hydrogen for energy storage, transportation, or industrial applications [1]. Currently, most hydrogen is produced via steam methane reforming; however, LTE can utilize renewable energy for the production of renewable hydrogen. In order to reach the United States Department of Energy target of hydrogen production cost below $2/kg, advancements in LTE systems are needed [2]. In addition to improvement in materials, significant cost reductions can be derived from improvements in manufacturing processes [3,4]. Thus, as polymer electrolyte membrane water electrolyzer (PEMWE) production increases in scale, high-volume roll-to-roll (R2R) manufacturing methods will be needed to meet both the volume and cost targets [5].

The membrane electrode assembly (MEA) is one of the key components of an LTE system that can be produced through R2R methods. For PEMWE, the most common MEA construction is the catalyst-coated membrane (CCM), where the anode and cathode catalyst layers are applied to the membrane, either through a transfer process or direct coating [6]. Alternatively, the catalyst can be applied to the porous transport layers (PTLs), though this is less common [6,7]. In a decal transfer process the

catalyst layer is applied to a decal substrate (e.g. polytetrafluoroethylene, polyimide, etc.) and then laminated to the membrane under high temperature and pressure [8–10]. Since the catalyst layers are applied to the membrane as dried layers, membrane swelling is eliminated. However, direct coating is desirable from a manufacturing perspective because it reduces processing steps, which should reduce overall production costs. The challenge with direct coating is that the water and alcohols commonly used as the dispersion media in catalyst inks swell the membrane [11].

For laboratory-scale MEAs, swelling can be mitigated by mechanically stabilizing the membrane on a heated vacuum plate while directly spraying the catalyst layer on the membrane. Some researchers have also developed alternatives like pre-swelling the membrane prior to direct coating to avoid swelling during coating, but these methods are not widely used [12,13]. Spray coating enables high uniformity and precise control of catalyst loading but is a slow process [14–17]. R2R spray coating of carbon nanotube supercapacitor electrodes has been demonstrated, but this method is still limited in terms of processing time and coating area to achieve target thickness [18,19].

R2R coating using methods like slot die and gravure coating offer significantly higher throughputs. These methods have previously been demonstrated for coating onto decals and diffusion media, but have not been used for direct membrane coating [20–23]. R2R direct coating of the membrane presents a challenge because a large amount of ink is applied to the substrate at once. Therefore, the interaction time between the solvent and the membrane is lengthier than it is for spray coating, which may result in increased solvent permeation and swelling of the membrane. Also, unlike in spray coating where the membrane can be mechanically stabilized during the ink deposition, excessive swelling of the membrane may present challenges for tensioning and web control as the membrane is conveyed

through the R2R line. Therefore, to enable R2R direct-membrane coating, the catalyst ink should be designed to minimize absorption into the membrane while maintaining acceptable wetting and coatability.

This study demonstrates R2R PEMWE CCM production through direct coating of an iridium oxide (IrO_2) catalyst layer onto the membrane. In development of this process, observation of the ink-membrane interaction is necessary because the membrane consists of hydrophilic and hydrophobic domains that exhibit different properties (swelling, permeation, etc.) for various water/alcohol dispersion media (DM) mixtures [24,25]. First, sessile-drop contact-angle experiments of pure DM i.e. without catalyst and Nafion ionomer, on the membrane were performed to characterize membrane wetting and permeation. The rheological characteristics of catalyst inks and their coating properties (thickness, uniformity) with various solids content and water-to-alcohol ratios were also investigated. The results of these experiments were used to down-select catalyst ink formulations for R2R slot-die coating experiments. The R2R-coated CCMs were characterized *in situ* for performance as PEMWEs.

2. Experimental section

2.1. Materials and ink formulation

Catalyst inks were prepared by mixing commercial iridium(IV) oxide catalyst powder (Premion™, 99.99% metal basis, Ir 84.5% min, Alfa Aesar Co. Ltd., Ward Hill, MA, USA) first with deionized water (18 MΩcm, Milli-Q), then adding the alcohol of interest, and lastly adding the ionomer dispersion. The alcohols used were methanol (99.9% assay, Avantor Inc., Radnor, PA, USA), ethanol (99.5% assay,

Sigma-Aldrich, LLC, St. Louis, MO, USA), 1-propanol (99.5% assay, EMD Millipore Corp., Billerica, MA, USA) and 2-propanol (99.5% assay, Fisher Scientific, Hampton, NH, USA). The water-to-alcohol mass ratios studied were 90:10, 75:25, 50:50, and 25:75. The IrO_2 concentration was studied at three levels: 10wt.%, 20wt.%, and 30wt.% relative to the final ink weight. The ionomer solution was a water-based Nafion dispersion (Nafion™ D1021, 1000 EW at 10wt.%, Ion Power Inc., New Castle, DE, USA). It was used to create a fixed ionomer to catalyst (I/Cat) ratio of 0.15 for all inks.

For small-scale experiments, the catalyst was dispersed using a previously established sonication procedure [26]. The blended inks were mixed with a probe sonicator at 12 J for 2 min (S-4000, QSONICA, LLC., Newton, CT, USA) and then mixed for 1 h by a bath sonicator (M-3800, Emerson Electric Co., Ltd., St. Louis, MO, USA) with ice water. The mixed inks were left overnight to stabilize ionomer-particle interactions and then sonicated in the bath sonicator on the next day for 10 min to eliminate particle agglomeration before measurement or coating. For sessile-drop measurements on membranes, pure solvent mixtures were used without catalyst and ionomer.

For R2R coating experiments, the same IrO_2 powder, ionomer solution, and water/1-propanol mixture conditions were used, and the blended inks were shear mixed in an ice water bath at 10,000 rpm for 15 min by a Turrax mixer (T25, IKA Works Inc., Wilmington, NC, USA). The mixed inks were stirred overnight with a magnetic stir bar to allow for degassing and dissipation of any bubbles before the coating experiment.

2.2. Coating

For small-scale trials, i.e. predominantly to study solvent/membrane interactions, the formulated inks were directly coated onto the membrane film (Nafion™ 212, 50.8-µm-thick, Ion Power, Inc., New Castle, DE, USA) with a number 12 Mayer rod (0.3 mm wire diameter). Before coating, the thin cover

sheet was removed from the Nafion membrane; however, the backer sheet was left attached. An automatic film applicator (QPI-AFA3800, Qualtech Products Industry, Denver, CO, USA) was used to produce a uniform sample. The translational speed of the Mayer rod was fixed to 35 mm/s. The coated samples were dried in a hot air oven (VWR International, LLC, Radnor, PA, USA) at 60 °C for 15 min. To prevent deformation of the sample during the coating, polyimide tape was applied to the four corners of the membrane substrate to maintain tension.

A commercial R2R system (Mini-Labo Deluxe, Mirwec Yasui Seki, Bloomington, IN, USA) (see Fig. 1 and Fig. S1) was used as a platform for large-area CCM production. For the R2R coating trials, a standard PEMWE membrane film (Nafion™ 117, 183-µm-thick, 200-mm-width, unsupported (no backing film), Ion Power, Inc., New Castle, DE, USA) was used, and the R2R direct-coated CCMs were compared with ultrasonically sprayed CCM-based PEMWEs using the same membrane. A sheet of the membrane film was spliced into a roll of 100-µm-thick polyester film to create a web long enough to completely thread the web path of the R2R system. The coating speed was 1 m/min and a tension of 13 N was applied to the web for stable coating. A slot die (Premier Dies Corporation, Chippewa Falls, WI, USA) was used for the continuous coating process. The die body gap (slot-gap) was 250 µm, the coating width was 8 cm, and the coating gap was 200-400 µm. The coating flow rate was 4 ml/min and lengths of approximately 1.2 m were coated for each ink condition to ensure a stable coating flow. The inks were fed to the die at a constant flow rate using a syringe pump (NE-1000, New Era Pump Systems Inc., Farmingdale, NY, USA). The coated film was dried in-line in two 1-m-long air-flotation oven sections. The first section was set to 80 °C and the second section was set to 100 °C, for a total drying time of 2 min at the 1 m/min coating speed. Lastly, for the purpose of PEMWE MEA fabrication and testing, a Pt on high-surface area carbon (46.6wt.% Pt, TEC10E50E, Tanaka Holdings Co., Ltd., Tokyo,

Japan) cathode was fabricated by ultrasonic spraying (ExactaCoat, Sono-Tek Corporation, Milton, NY, USA) onto the opposite side of the membrane following R2R coating of the anode. The cathode ionomer/carbon ratio was 0.5 and the catalyst loading was 0.16 mg_{Pt}/cm^2, as measured using an X-ray fluorescence (XRF) spectrometer (Fischerscope XDV-SDD, Fischer Technology Inc., Windsor, CT, USA). Further details on the preparation of the Pt/HSC ink can be found in the literature [14].

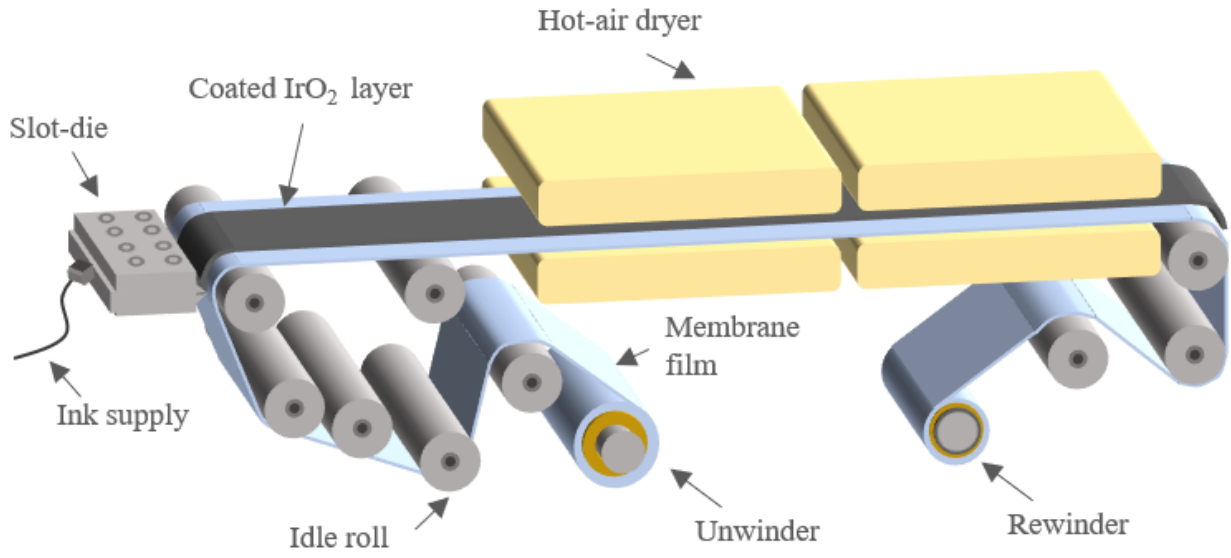

Fig. 1. Schematic of the process for R2R direct catalyst layer coating onto membrane.

2.3. Characterizations

The contact angle of the water/alcohol DM on the membrane was measured as a function of time using a drop shape analyzer (DSA 100, Krüss GmbH, Hamburg, Germany). A 3 µl droplet of solution was generated on a 1 mm diameter blunt needle. The sample stage with Nafion 212 membrane was then moved towards the pendant drop to detach it from the needle and form a sessile drop on the membrane. The Nafion 212 membrane was used because it is adhered to a backing sheet which mechanically stabilizes the membrane during the measurement. The drop shape was recorded, and the contact angle was measured for 200 s from the moment the sessile drop was formed. One thousand

frames were captured during the 200 s measurement. Three drop-aging measurements were made for each solution and the mean and standard deviation values are reported. The surface tension of the prepared ink was also measured with a pendant drop using the same system. A 5-µl-droplet was generated for the measurement on a blunt needle with a diameter of 1.8 mm. The mean and standard deviation values of the five surface-tension measurements for each ink are reported.

Steady-shear viscosities of the formulated inks were measured using a stress-controlled rheometer (Haake Mars 60, Thermo Fisher Scientific Inc., Waltham, MA, USA). The measurements were conducted using a 35 mm diameter stainless steel parallel plate with a gap of 500 µm. Temperature was controlled at 25 °C for stable measurements and a solvent saturation trap filled with the same water/alcohol as the catalyst ink was used to prevent evaporation from the ink. The shear viscosities were measured in the shear rate region from 1000 to 1/s from high to low shear rate. All measurements were performed after a pre-shearing of the ink at 500 1/s for 30 s and then a 1 min rest.

The surface morphology of the CCMs was measured using an optical microscope (VHX-5000, Keyence Corp., Osaka, Japan). Measurements were taken at 200x and 1000x magnifications using a VH-Z100R lens. XRF was used to confirm loading of the coated IrO_2 layer. Ir mapping was performed on the coated samples. For each small scale sample, nine points were measured in a 4 × 4 cm^2 area. The mean values reported are the mean of at least 3 individual coated samples. For the R2R coated samples, 32 points in a 6 × 50 cm^2 area for R2R coated samples. Each point was measured for 30 s.

2.4. Electrochemical testing

The R2R-processed CCMs were evaluated in single cell PEMWE hardware. Polytetrafluoroethylene-free carbon paper AvCarb MGL370 (Fuel Cell Earth LLC, Woburn, MA, USA) with a nominal thickness of

370 µm and a porosity of 78% was used as the porous transport layers for both anode and cathode [27]. The 25 cm^2 hardware featured triple-serpentine graphite bipolar plates. DI water (~18 MΩ·cm) was pumped at 80 °C and a water flow rate of 80 ml/min was used on both anode and cathode. The anode and cathode backpressures were both at ambient pressure, i.e. approximately 83 kPa based on the laboratory's elevation. For cell conditioning, voltages of 1.5, 1.6, and 1.7 V were applied for 30 min, 30 min, and 2 h, respectively. The polarization curves contained an up-scan (anodic) and a down-scan (cathodic) and were controlled in current-controlled mode (galvanostatic) with a power supply (HP6031A). The resulting voltages were measured with a multimeter (Keithley 2000). The current range was 0.02 – 2.5 A/cm^2 with a voltage limit of 2.5 V. The step sizes were below 80 mA/cm^2 between 0.02 A/cm^2 – 0.4 A/cm^2, 100 mA/cm^2 between 0.4 A/cm^2 – 1 A/cm^2, and finally 250 mA/cm^2 between 1 – 2.5 A/cm^2. The cell was held at each current density for 2 minutes and the reported cell voltage was obtained by averaging the last 60-second data of each step from both up-scan and down-scan. Electrochemical impedance spectroscopy (EIS) was measured using a potentiostat system (Gamry Reference 3000 and 30k booster, Gamry Instruments, Warminster, PA, USA). The applied frequencies ranged from 300 kHz to 500 mHz. Full EIS scans were conducted after every up-scan current step within 0.02-1.2 A/cm^2. The high frequency resistance (HFR) results were extracted from the x-intercept of the spectra in the Nyquist plots.

3. Results and discussion

In order to best design the catalyst ink for direct coating on the membrane, an improved understanding of the interactions between the DM and the membrane is necessary. Understanding

these interactions is complicated due to the heterogeneous structure of the membrane. In a perfluorinated sulfonic acid membrane like Nafion, the tetrafluoroethylene backbone forms a continuous hydrophobic phase surrounding the hydrophilic domains formed by the sulfonic acid side chains [24]. Because of this structure, the membrane can exhibit different swelling and permeation behaviors in different mixtures of water and alcohol, as each constituent of the mixture can interact differently with the hydrophobic and hydrophilic domains [11].

Figure 2 presents the sessile drop contact angle data for different mixtures of water and alcohols on a 50 µm Nafion membrane as a function of time. Figure 2(a) shows images of the drop shape at various time points for mixtures of water and 1-propanol. The measured contact angle as a function of time for all alcohols and water/alcohol ratios are shown in Figs. 2(b)-(e). As expected, the greater the alcohol content in the DM, the lower the surface tension of the liquid [28]. There is also a decrease in contact angle with decreasing alcohol polarity, from methanol to 2-propanol. For water/1-propanol, the initial contact angle decreases from 88.6° for a 90:10 mixture to 29.7° for a 25:75 mixture, as shown in Fig. 2(a). However, interestingly the 50:50 water/1-propanol mixture in Fig. 2(a) shows the lowest initial contact angle of 21° compared to 29.7° for the 25:75 mixture. Additionally for this mixture, the sessile drop penetrates into the membrane in about 50 s. Similar contact angle change and droplet penetration were also observed for the water/2-propanol mixture in Fig. 2(c). This behavior was not observed with methanol or ethanol, as shown in Figures 2(d) and (e), which display monotonic decreases in contact angle with increasing alcohol content.

It is suspected that this unique result is due to the interactions between the hydrophobic and hydrophilic domains of the membrane and the water and propanol molecules of the DM. The relative polarities of water, methanol, ethanol, 1-propanol and 2-propanol are 1, 0.762, 0.654, and 0.617, and

0.546, respectively [29]. It has previously been shown that increasing the number of carbons in primary alcohols (thus decreasing polarity) increases the swelling of Nafion membranes [11]. At 50:50 water/propanol, it seems the mixture is such that the polar and non-polar molecules rapidly swell both the hydrophilic and hydrophobic domains of the Nafion membrane [24,30]. At other water/propanol ratios the mixture is either too polar or too nonpolar to swell the whole membrane and instead primarily swells the hydrophilic or hydrophobic domains, respectively. Similarly, the absence of this rapid swelling behavior for the water/methanol or water/ethanol mixtures is likely due to the higher polarity of these shorter alcohols making all mixtures too polar to significantly swell the hydrophobic domains in the timescale measured here.

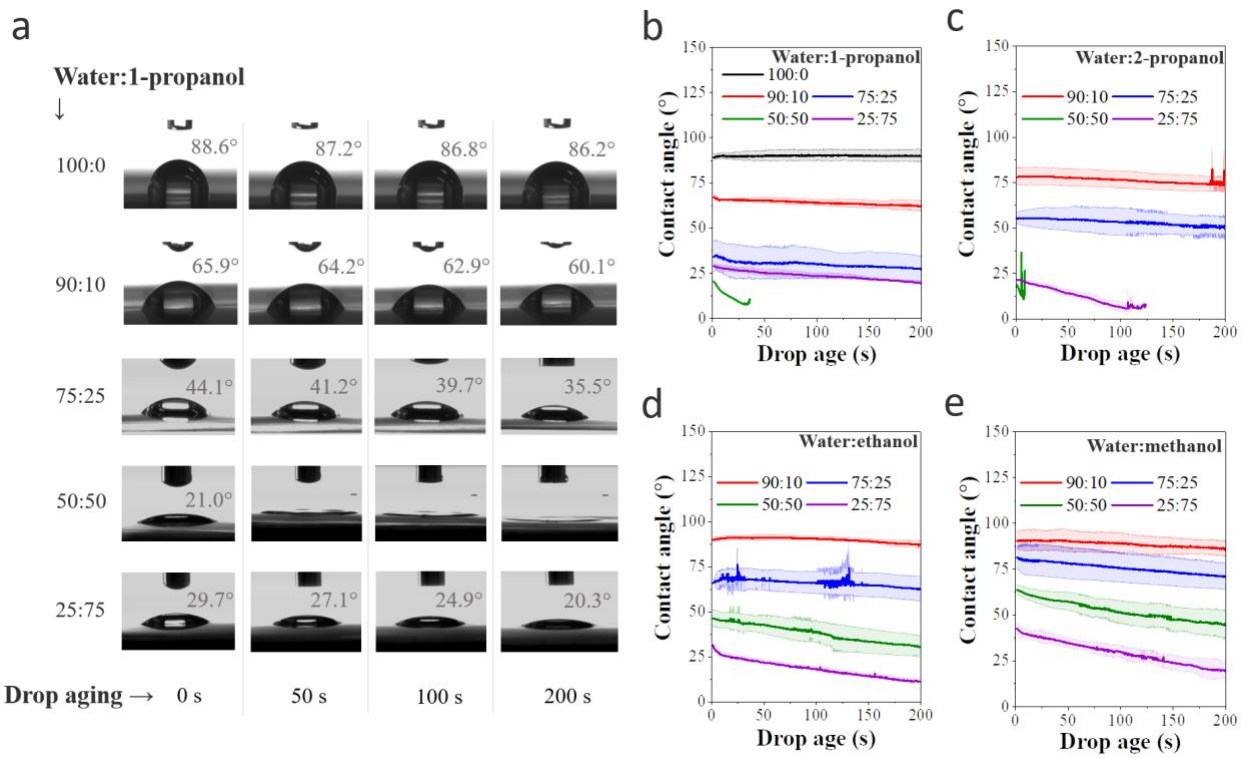

Fig. 2. Contact angle measurements of water and alcohol mixtures on Nafion 212 membrane as drop aging: (a) Photos of sessile drops at different times after formation for different water/1-propanol mixtures - 100:0 (only water), 90:10, 75:25, 50:50, and 25:75. Measured contact angle data as a function of time with different mixtures of water and (b) 1-propanol, (c) 2-propanol (d) ethanol, and (e) methanol. In the results of 50:50 ratio condition of (b) and (c), only single measurement data was shown because the very low contact angle resulted in high uncertainty of the measurement. If the

sessile drop spreads too much or is absorbed into the membrane, there is a difficulty in contact angle fitting.

These data also provides a measure of the absorption rate of the DM mixture into the membrane. The change in contact angle for the drops shown in Fig. 2(a) can be used as a proxy for absorption. For the 100:0 water/1-propanol mixture the contact angle decreases 0.4° from 0 s to 200 s. For the 90:10 mixture the decrease is larger, 5.8°. It decreases even more, 8.6°, for the 75:25 mixture, and comparably, 9.4°, for the 25:75 mixture. For the 50:50 mixture, however, the absorption is too rapid for comparison. These data show that the absorption rate increases as the 1-propanol content is increased up to its maximum at 50% and then decreases with further increases in 1-propanol.

The sessile-drop experiments indicate that the absorption rate of the DM into the membrane is generally slow. Over the 200 s measured, which is on the order of magnitude of the coating and drying process on our coating line, in almost all cases the drop shape and volume change only slightly. Only for the 50:50 water/propanol cases do we observe rapid absorption of the DM. This suggests that in most cases the evaporation rate of the solvent in the drying ovens will be greater than the absorption rate into the membrane. It is important to note that in the R2R coating experiment in this study, the distance between the coating location and the drying oven is about 50 cm, and thus the time to the drying section after coating is about 30 s at a web speed of 1 m/min. The membrane swelling may be less of a concern in a scaled-up and equipment-optimized industrial coating line given that the time from coating to drying could decrease further as the coating speed increases and/or if the physical distance between the coating head and the drying oven is minimized.

Based on the observed absorption and wetting behavior, the 1-propanol- and ethanol-based DM were selected for the coating experiments because they showed good wetting of the membrane

(contact angle < 90°). Previous work [11] and our experimental results have indicated that these liquids can permeate and swell the membrane. Nevertheless, as discussed above, the swelling of the membrane was expected to be limited considering the length of time from the coating section to the drying section in our R2R system.

In order to better predict and understand coating phenomena, the steady-shear rheology of the catalyst inks was measured. For catalyst and ionomer dispersions, the interactions between components can be assessed through rheological measurements [26,31]. Alcohol-free IrO_2 dispersions were not considered in this study because such inks resulted in severe dewetting on the membrane due to high surface tension (see Fig. S2). Figure 3 shows the measured steady-shear viscosities of the formulated inks with water/1-propanol dispersion media. The inks are primarily Newtonian in the shear rate range of 10 to 1000 1/s.

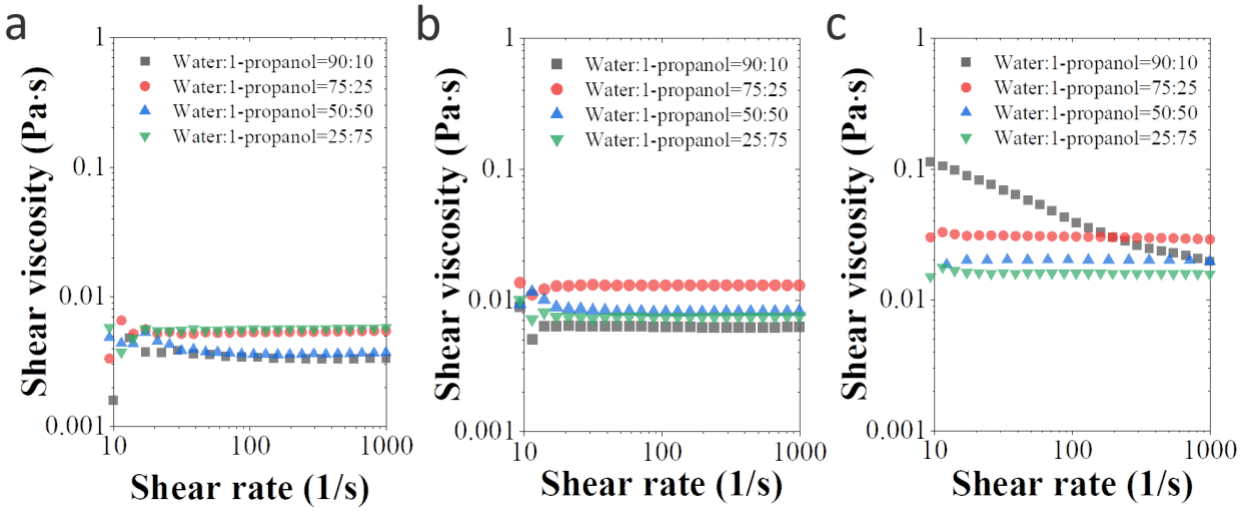

Fig. 3. Steady-shear viscosity data for different water/1-propanol ratios of (a) 10wt.% IrO_2, (b) 20wt.% IrO_2, and (c) 30wt.% IrO_2 dispersions.

Shear thinning behavior is only observed in the 90:10 ink with 30wt.% IrO_2, as indicated by the decreasing shear viscosity in Fig. 3(c). At higher alcohol content the 30wt.% IrO_2 inks remain

Newtonian. In particle dispersions, shear thinning behavior is associated with weakly agglomerated particles [32]. In contrast, Newtonian rheology is the result of well dispersed particles. We have previously shown that IrO_2 catalyst particles tend to agglomerate in the absence of ionomer and that under certain ink formulations the addition of ionomer stabilizes the particles against agglomeration [26]. The change from Newtonian to shear thinning at 30 wt.% in the 90:10 dispersion indicates that under these conditions the catalyst particles have agglomerated. This increases the effective volume fraction of the solid leading to the increase in viscosity [33,34]. That the change in rheology is dependent on the water-to-alcohol ratio indicates that there are changes in agglomeration depending on the ink formulation. Likely the high water content of the 90:10 ink leads to a destabilization of the dispersion that results in the agglomeration that is evident here. The Newtonian behavior of the ink with higher alcohol content indicate that, in these formulations, the particles are more dispersed.

IrO_2 solutions with water/ethanol DM were also evaluated, with results shown in Fig. S3. For these inks shear thinning behavior begins to occur at 20wt.%. Because shear thinning is observed at a lower solids content, this indicates the catalyst is less dispersed in these water/ethanol mixtures than it was in the water/1-propanol mixtures, where shear thinning behavior was not observed until 30wt.% IrO_2. This is consistent with the analysis that the high polarity of the 90:10 water/1-propanol ratio ink was leading to less stability than in inks with higher alcohol content. Because ethanol is more polar than 1-propanol it is reasonable that agglomeration would be observed at lower concentration and higher alcohol content.

Figure 4 displays the surface tension data of inks as a function of catalyst concentration and water/1-propanol ratio. For the 90:10 inks, the surface tension decreases from 31 to 26 mN/m as the IrO_2 concentration increases from 10wt.% to 30wt.%. This trend is consistent for all water/1-propanol

ratios. As the IrO_2 catalyst content increases, the ratio of solvent molecules to catalyst particles in the solution decreases. Given that the catalyst particles are orders of magnitude larger than the solvent molecules, the solvent is increasingly replaced by catalyst and ionomer particles at the solvent-gas interface, leading to the reduction in surface tension [35].

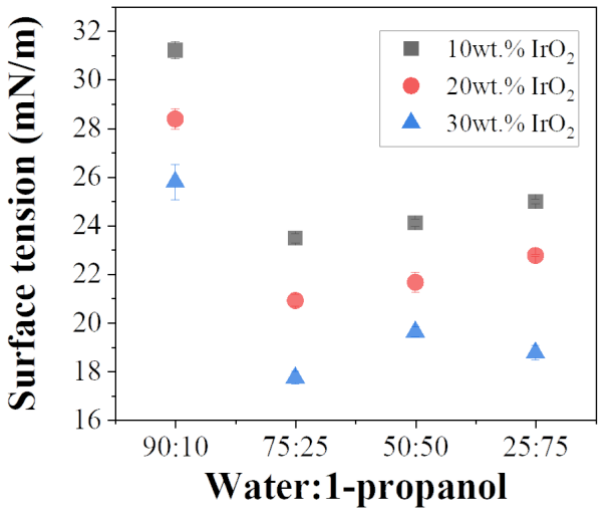

Fig. 4. Surface tension for different IrO_2 concentrations as a function of water/1-propanol ratio.

Before performing R2R large-area coating, lab-scale coating experiments were conducted to verify the coatability of each ink under various formulation conditions. Figure 5 shows photographs of the coated films. Most of the catalyst layers are visually uniform. In the case of the 10wt.% IrO_2 dispersion [Figs. 5(a-1) to (a-4)], variations in coating thickness can be visually seen as a function of 1-propanol content. These coatings also exhibit the most irregularities: for example, voids can be seen in the coatings due to dewetting. The catalyst layers cast from the 20wt.% and 30wt.% IrO_2 dispersions (Figs. 5(b) and (c)) all show similar visual uniformity, i.e. they all appear as opaque, black coatings. And, as would be expected from the surface tension data in Figure 4, irregularities in the high-solids coatings were not observed due to the increased resistance to dewetting.

In contrast to the water/1-propanol based inks, the coating surface with water/ethanol DM-based IrO_2 solution showed higher irregularity with wave patterns on the coating surface (see Fig. S4). This may be due to poorer dispersion of the ink, as indicated by the rheological measurements, or due to the higher surface tension of the water/ethanol inks not wetting the membrane as well as the water/1-propanol inks.

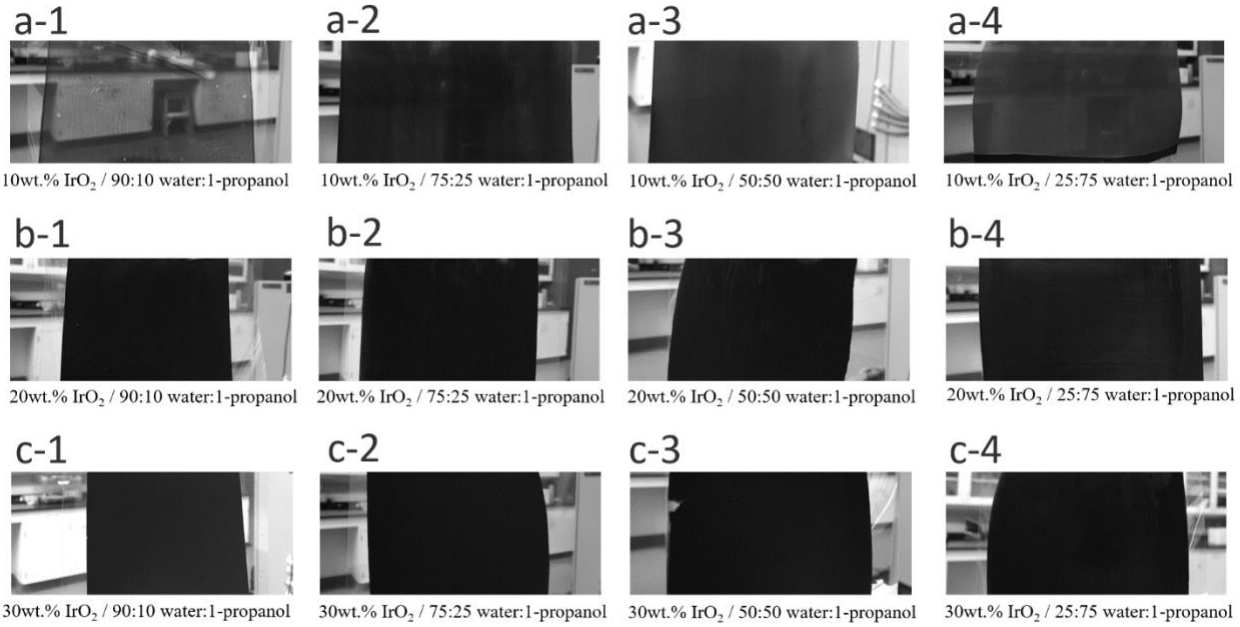

Fig. 5. Direct coated IrO2 electrodes on Nafion 212 membrane: The inks used (a) 10wt.% IrO2, (b) 20wt.% IrO2, and (c) 30wt.% IrO2 dispersions. The caption number from 1 to 4 denotes the water/1-propanol ratio of the ink of 90:10, 75:25, 50:50, and 25:75, respectively.

Table 1 shows the Ir loadings of the coated catalyst layers measured by XRF. It provides the measured average and standard deviation of Ir loading values for each of the 12 CCMs. The reported values represent the mean loading and its standard deviation of three separate coatings at each condition.

Table 1. Measured Ir loading of the CCMs prepared using inks with different water/1-propanol ratios and IrO_2 solids content.

Measured Ir loading (mg/cm²)		**IrO_2 contents in the ink**		
		10wt.%	20wt.%	30wt.%
Water:1-propanol	90:10	0.09±0.006	0.43±0.049	0.95±0.376

	75:25	0.29±0.055	0.50±0.157	0.83±0.157
	50:50	0.26±0.031	0.62±0.444	1.33±0.603
	25:75	0.19±0.012	0.39±0.052	0.50±0.071

The data generally indicate a maximum loading for the 50:50 inks, except for the 10wt.% IrO_2 cases where the 75:25 and 50:50 inks result in loadings that are within error of each other. As discussed above relative to Figs. 3 and 4, the 50:50 inks did not show significantly higher shear viscosity or surface tension values, which would be expected to alter the coating physics, than the other inks. Therefore, the high variance in Ir loading in catalyst layers from the 50:50 inks can be presumed to be due to the rapid permeation of this DM mixture into the membrane that was observed with the contact angle measurements and discussed using Fig. 2(a). The rapid permeation would likely cause the membrane to deform and move away from the coating rod in certain locations leading to a thicker coating in these areas. This hypothesis is supported by the results of the water/ethanol DM-based IrO_2 inks, which do not show such large loading variations. As shown in Fig. 2(d), rapid permeation into the membrane did not occur for the 50:50 water/ethanol mixture. Accordingly, the loading deviation for catalyst layers from these inks was not significantly different from the other inks (see Table S1).

Figure 6 shows microscope images of the CCMs at 1000x magnification (see Fig. S5 for microscope images at 200x). The coatings with the most uniform visual appearance are found in inks with 75:25 and 50:50 water/1-propanol mixtures. Generally, as the solid content increases, at a given water/1-propanol ratio, the coating quality improves. Despite the low standard deviation of loading for the ink with 10wt.% IrO_2 dispersions, the result from the 90:10 water/1-propanol ratio ink shows a very heterogeneous microstructure, which is confirmed by several voids and clumps of catalyst, as shown in Fig. 6(a-1). The rheological measurements indicated that this ratio leads to a poorer dispersion of

particles, which seems to have persisted in the dry film. Similarly, heterogeneous coatings are observed at the 25:75 water/1-propanol ratio with voids in the coating layer, as shown in Fig. 6(a-4).

In several of the films cracking occurred. The degree of cracking appears to increase with 1-propanol content. For example, the 20wt.% IrO_2, 90:10 water/1-propanol ratio ink did not result in any cracking, whereas the 25:75 water/1-propanol ratio ink mixture did. As the solids content is increased to 30wt.% IrO_2, all of the catalyst layers develop some cracking. This indicates that all these thicker films are above their critical cracking thickness [36]. Interestingly, the catalyst layers from the 25:75 inks show cracking at loadings that are crack free for other inks indicating that the ink formulation, not just the layer thickness, influences cracking behavior.

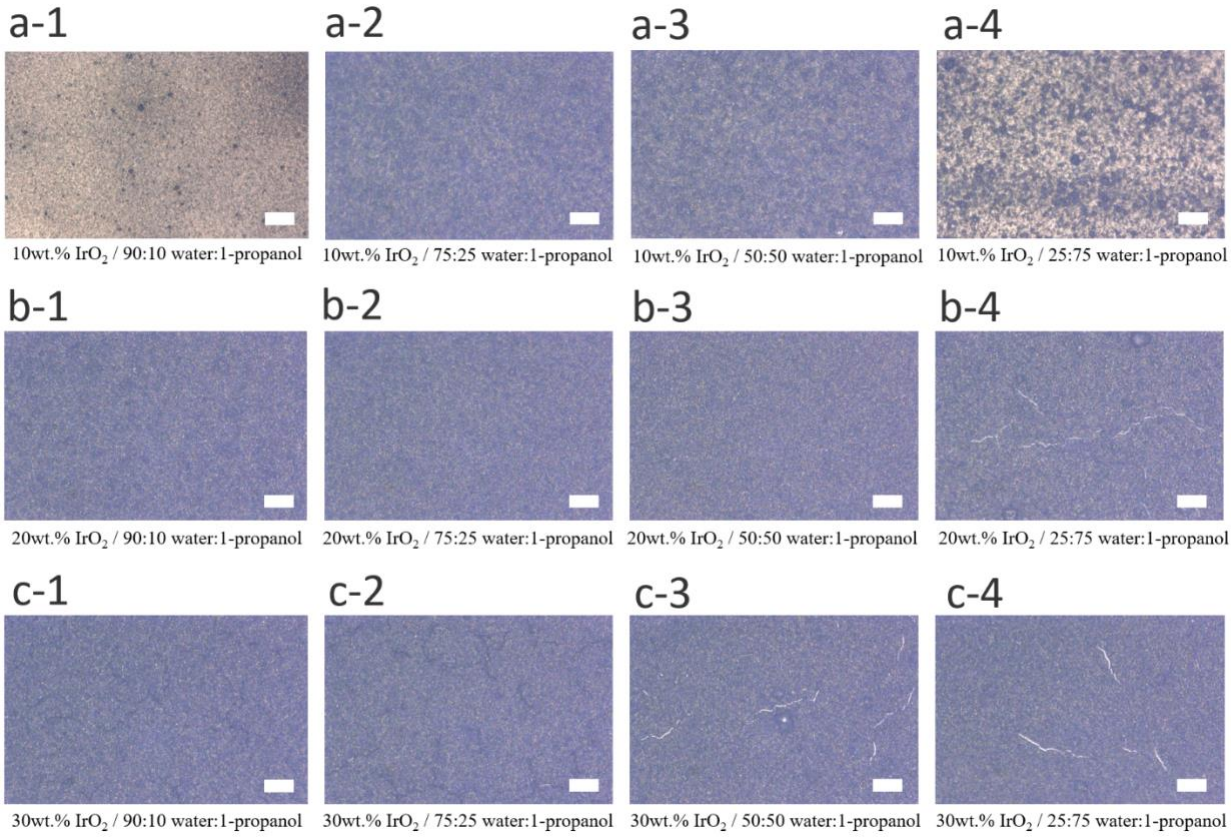

Fig. 6. Microscopic images catalyst layer top surface from water/1-propanol inks: the inks used (a) 10wt.% IrO_2, (b) 20wt.% IrO_2, and (c) 30wt.% IrO_2 dispersions. The caption number from 1 to 4 denotes that the water/1-propanol ratio of the ink are 90:10, 75:25, 50:50, and 25:75. Scale bar is 30 µm.

Microscopy images for catalyst layers cast from water/ethanol DM mixtures are shown in Figs. S6 and S7. Unlike the 1-propanol cases, a large number of agglomerates are observed in the 10wt.% dispersions regardless of ethanol content. Cracks begin to occur at 75% ethanol content of 20wt.% ink, similar to the 1-propanol case.

Based on the results of DM/membrane interactions, ink rheology, and lab-scale catalyst-layer coating results we down-selected ink formulations to be used in the R2R experiment to two inks: 90:10 and 75:25 water/1-propanol . Water/1-propanol inks were selected because these resulted in better dispersion of the catalyst than water/ethanol. The 90:10 ratio was selected because it should minimize interactions between the ink and the membrane. The 75:25 mixture was selected because it resulted in a better dispersion of the catalyst particles. The IrO_2 was fixed at 20wt.% IrO_2 as small-scale coatings at this concentration showed high coating uniformity.

These inks were slot-die coated onto Nafion 117 membrane using the R2R coating system. Both inks resulted in some deformation of the membrane directly after the coating die due to DM-induced swelling. As shown in Fig. 7(a), once the coated membrane exited the oven, much of the deformation was observed to have significantly diminished. This was not observed for lab-scale samples that were dried in an oven. This suggests that the combination of heat and web tension was able to remove some of the swelling-induced wrinkling of the membrane. The direct-coated IrO_2 catalyst layer had the same adhesion to the membrane as that of an ultrasonically sprayed CCM, with both having 3 – 5% of the material removed under the ASTM D3359 standard protocol. These coatings had, like the lab-scale samples, visibly uniform surfaces as shown in the microscopic images in Figs. 7(b) and (c) (see Fig. S8 for larger magnification of microscopic images). Anode catalyst loadings of 1.06±0.084 and 0.85±0.047 mg_{Ir}/cm^2 were obtained for the 90:10 and 75:25 water to 1-propanol ratios, respectively. These

coatings have lower loading variation than the small-scale rod coated samples, likely because slot-die coating is a steady-state (pre-metered) coating process as opposed to the less-precisely controlled small-scale rod-coating process.

As discussed in the introduction, R2R processes like slot-die coating are expected to have much greater throughput than lab-scale or other large-scale processes. For example, in the case of our lab-scale ultrasonic spray coating, it takes about an hour and a half to coat an area of 100 cm^2 with an Ir loading of 1 mg/cm^2. With R2R slot-die coating, it only takes 7.5 s to achieve this loading at a coating speed of 1 m/min with a coating width of 8 cm. This constitutes 720 times increase in throughput compared to the spray coating example. Furthermore, this increase in throughput is expected to be even greater when coating width and coating speed are further increased during equipment-optimized fully industrial R2R coating.

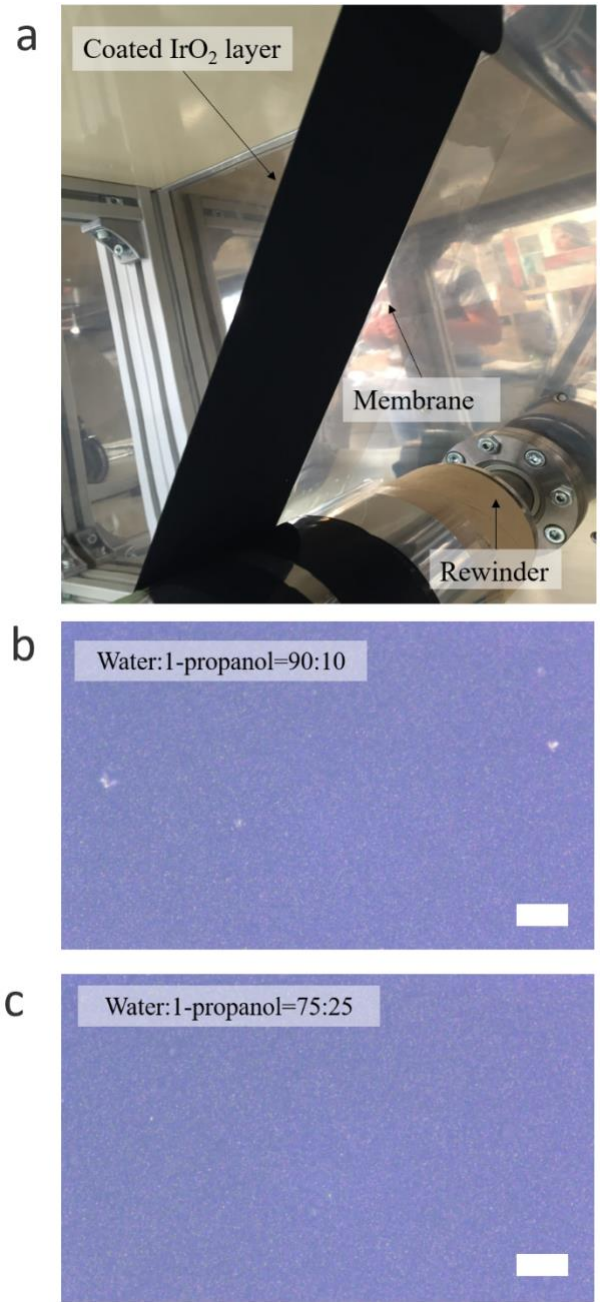

Fig. 7. R2R production of CCMs: (a) photograph of the direct coated IrO_2 catalyst layer on Nafion 117 membrane in the rewinding zone, and microscope images of the R2R-coated samples with water/1-propanol ratios of (b) 90:10 and (c) 75:25 (scale bar: 30 μm).

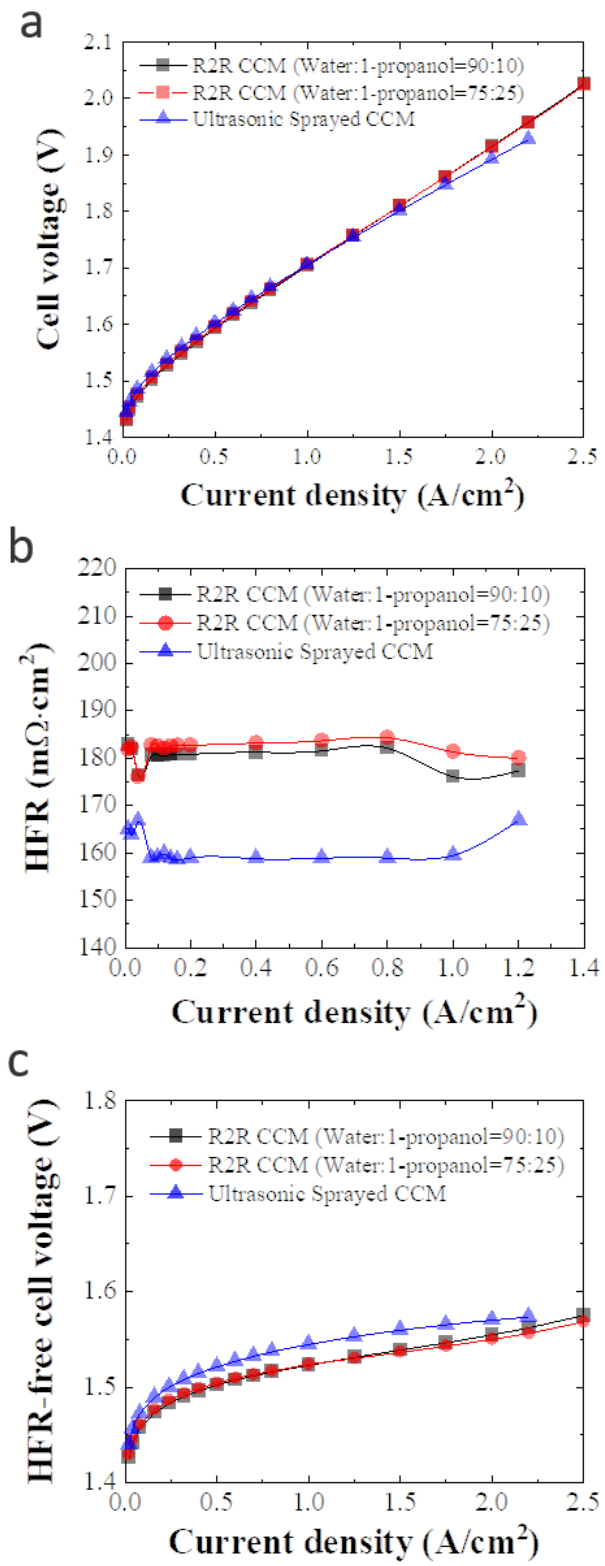

Fig. 8. Electrochemical test results comparing R2R processed [Water:1-propanol=90:10 and 75:25] and ultrasonic sprayed CCMs: (a) ambient-pressure polarization curves for MEAs with pumping DI water at 80 °C and 80 ml/min of water flow rate (b) HFR data (c) HFR-free performance data.

Figure 8 shows (a) ambient-pressure polarization curves, (b) high frequency resistance (HFR), and (c) HFR-free polarization curves of the R2R-coated anodes and an ultrasonically sprayed anode with similar 1.2 mg_{Ir}/cm^2 loading. The two R2R-coated CCMs perform identically and, critically are very similar to the spray coated MEA. The R2R samples show better performance than the spray-coated sample at current densities below 1.25 A/cm^2. However, this trend reverses at current densities above 1.25 A/cm^2. For example, at 2 A/cm^2, the cell voltages for the two coated samples and the sprayed sample are 1.91 V and 1.89 V, respectively. This result is consistent with the obtained HFR values, which are shown in Fig. 8(b), and indicate that the R2R coated samples have an about 13% increased cell resistance (see Fig. S9 for EIS data). The HFR-free polarization curves shown in Figure 8(c) in conjunction with the other data suggests there may be some kinetic advantages and some interfacial deficiencies of slot-die coating compared to spray coating, but further study of the interface and the electrode morphology is needed to verify this. As the major part of the HFR is typically associated with the membrane, the variations in MEA performance and HFR could also result from slight differences in membrane thickness that occur due to dimensional changes during the coating process [37].

Interestingly there is no apparent effect of the water/1-propanol ratio on performance. Previous measurements of spray-coated MEAs with 0.1 mg_{Ir}/cm^2 loadings showed increasing the water/1-propanol ratio resulted in a decrease in performance [38]. This may be an effect that is specific to low-loaded samples or the coating method. These data also do not suggest there is any impact of different membrane swelling on initial performance. It is possible that differences in swelling could induce stresses in the membrane that would lead to failures or changes in degradation rate under extended operation. However, because the membrane will be fully hydrated and swollen during operation, which would likely reduce residual stresses in the membrane during operation, this may not prove to

be an issue. Extended testing will be needed to understand whether or not there is an impact on durability.

4. Conclusion

This work demonstrates the successful direct coating of IrO2 catalyst layers on perfluorinated membrane using an industrial coating method. To enable this, the catalyst ink must be formulated with several considerations in mind: minimal swelling of the membrane, good wetting of the membrane, and well dispersed catalyst particles. All of these conditions must be satisfied to enable a uniformly coated, high-performance catalyst layer. Ex-situ studies indicated that most mixtures of water and alcohols are not rapidly absorbed by the membrane. However, in some cases, while an ink might not be rapidly absorbed by the membrane, poor catalyst dispersion may lead to coating defects or a heterogenous microstructure. Inks with water/ethanol DM had favorable interactions with the membrane, yet they tended to result in poor coatings. Mixtures of water and 1-propanol were able to satisfy all of the above criteria, specifically 90:10 and 75:25 water/1-propanol mixtures. These mixtures showed slow absorption by the membrane, low contact angle, and good dispersion of the catalyst particles. These ink formulations were used to successfully slot-die coat anode electrodes onto the membrane in a single step R2R process. In situ performance of the resulting CCMs showed that these MEAs performed similarly to lab-scale, spray-coated MEAs, though there were some small differences that warrant further investigation. By fabricating high performance catalyst layers through directly coating on the membrane we have, compared to our standard lab-scale spray coating, increased the throughput of CCM fabrication by more than 500x. In a true industrial setting, this increase in

throughput is expected to be even greater. Additionally, this work shows that it should be possible to eliminate the decal transfer processes that is commonly used today. Both of these factors will lead to reduced catalyst layer production costs in PEMWE manufacturing. The learnings from this study are also relevant to fuel cells and CO_2 electrolysis, given the similarity in materials and production methods.

CRediT authorship contribution statement

Janghoon Park: Methodology, Investigation, Validation, Formal analysis, Data curation, Writing - original draft, Visualization. **Zhenye Kang**: Data curation, Formal analysis, Writing - review & editing, Visualization. **Guido Bender**: Formal analysis, Supervision, Writing - review & editing. **Michael Ulsh**: Conceptualization, Writing - review & editing, Supervision, Project administration, Funding acquisition. **Scott A. Mauger**: Conceptualization, Writing - review & editing, Supervision, Project administration, Funding acquisition.

Acknowledgements

This work was authored by the National Renewable Energy Laboratory, operated by the Alliance for Sustainable Energy, LLC, for the U.S. Department of Energy (DOE) under Contract No. DE-AC36-08GO28308. Funding provided by the U.S. Department of Energy, Office of Energy Efficiency and Renewable Energy, Hydrogen and Fuel Cell Technologies Office. The views expressed in the article do not necessarily represent the views of the DOE or the U.S. Government.

Appendix A.

Supplementary data Supplementary data to this article can be found online at xxx

ORCID

Janghoon Park: 0000-0002-5897-4241

Zhenye Kang: 0000-0002-1731-0705

Guido Bender: 0000-0003-3777-4707

Michael Ulsh: 0000-0003-3725-8032

Scott A. Mauger: 0000-0003-2787-5029

REFERENCES

[1] B. Pivovar, N. Rustagi, S. Satyapal, Hydrogen at scale (H2@ scale): key to a clean, economic, and sustainable energy system, Electrochem. Soc. Interface. 27 (2018) 47–52.
[2] E.L. Miller, D. Papageorgopoulos, N. Stetson, K. Randolph, D. Peterson, K. Cierpik-Gold, A. Wilson, V. Trejos, J.C. Gomez, N. Rustagi, US Department of energy hydrogen and fuel cells program: progress, challenges and future directions, MRS Adv. 1 (2016) 2839–2855.
[3] C. Daniel, D. Wood III, G. Krumdick, M. Ulsh, V. Battaglia, F. Crowson, Roll-to-Roll Advanced Materials Manufacturing DOE Laboratory Collaboration-FY2018 Final Report, Oak Ridge National Lab.(ORNL), Oak Ridge, TN (United States), 2019.
[4] U.S. Department of Energy, Roll-to-Roll Processing, in: Quadrenial Technol. Rev. 2015, n.d. https://www.energy.gov/sites/prod/files/2016/02/f30/QTR2015-6K-Roll-to-Roll-Processing.pdf.
[5] A. Mayyas, M. Mann, Emerging Manufacturing Technologies for Fuel Cells and Electrolyzers, Procedia Manuf. 33 (2019) 508–515. https://doi.org/10.1016/j.promfg.2019.04.063.
[6] M. Carmo, D.L. Fritz, J. Mergel, D. Stolten, A comprehensive review on PEM water electrolysis, Int. J. Hydrog. Energy. 38 (2013) 4901–4934. https://doi.org/10.1016/j.ijhydene.2013.01.151.
[7] M. Bühler, P. Holzapfel, D. McLaughlin, S. Thiele, From Catalyst Coated Membranes to Porous Transport Electrode Based Configurations in PEM Water Electrolyzers, J. Electrochem. Soc. 166 (2019) F1070–F1078. https://doi.org/10.1149/2.0581914jes.
[8] Z. Wei, K. Su, S. Sui, A. He, S. Du, High performance polymer electrolyte membrane fuel cells (PEMFCs) with gradient Pt nanowire cathodes prepared by decal transfer method, Int. J. Hydrog. Energy. 40 (2015) 3068–3074.
[9] M. Bernt, A. Siebel, H.A. Gasteiger, Analysis of voltage losses in PEM water electrolyzers with low platinum group metal loadings, J. Electrochem. Soc. 165 (2018) F305–F314.
[10] M.S. Wilson, S. Gottesfeld, Thin-film catalyst layers for polymer electrolyte fuel cell electrodes, J. Appl. Electrochem. 22 (1992) 1–7. https://doi.org/10.1007/BF01093004.
[11] Y.D. Yi, Y.C. Bae, Swelling behaviors of proton exchange membranes in alcohols, Polymer. 130 (2017) 112–123. https://doi.org/10.1016/j.polymer.2017.09.069.

[12] C. Hsu, C. Wan, An innovative process for PEMFC electrodes using the expansion of Nafion film, J. Power Sources. 115 (2003) 268–273.
[13] W. Wang, S. Chen, J. Li, W. Wang, Fabrication of catalyst coated membrane with screen printing method in a proton exchange membrane fuel cell, Int. J. Hydrog. Energy. 40 (2015) 4649–4658.
[14] M. Wang, J.H. Park, S. Kabir, K.C. Neyerlin, N.N. Kariuki, H. Lv, V.R. Stamenkovic, D.J. Myers, M. Ulsh, S.A. Mauger, Impact of Catalyst Ink Dispersing Methodology on Fuel Cell Performance Using in-Situ X-ray Scattering, ACS Appl. Energy Mater. (2019).
[15] S.A. Mauger, J.R. Pfeilsticker, M. Wang, S. Medina, A. Yang-Neyerlin, K.C. Neyerlin, C. Stetson, S. Pylypenko, M. Ulsh, Fabrication of high-performance gas-diffusion-electrode based membrane-electrode assemblies, J. Power Sources. 450 (2020) 227581.
[16] M. Wang, S. Medina, J.R. Pfeilsticker, S. Pylypenko, M. Ulsh, S.A. Mauger, Impact of Microporous Layer Roughness on Gas-Diffusion-Electrode-Based Polymer Electrolyte Membrane Fuel Cell Performance, ACS Appl. Energy Mater. 2 (2019) 7757–7761.
[17] S.M. Alia, S. Stariha, R.L. Borup, Electrolyzer Durability at Low Catalyst Loading and with Dynamic Operation, J. Electrochem. Soc. 166 (2019) F1164. https://doi.org/10.1149/2.0231915jes.
[18] M. Karakaya, J. Zhu, A.J. Raghavendra, R. Podila, S.G. Parler Jr, J.P. Kaplan, A.M. Rao, Roll-to-roll production of spray coated N-doped carbon nanotube electrodes for supercapacitors, Appl. Phys. Lett. 105 (2014) 263103.
[19] M. Bühler, C. Klose, F. Hegge, T. Lickert, S. Thiele, A Novel Fabrication Technique for Electrodes of PEM Water Electrolyzers, ECS Trans. 80 (2017) 1069.
[20] M. Bodner, H.R. García, T. Steenberg, C. Terkelsen, S.M. Alfaro, G.S. Avcioglu, A. Vassiliev, S. Primdahl, H.A. Hjuler, Enabling industrial production of electrodes by use of slot-die coating for HT-PEM fuel cells, Int. J. Hydrog. Energy. 44 (2019) 12793–12801.
[21] A. Glüsen, M. Müller, D. Stolten, Slot-Die Coating: A New Preparation Method for Direct Methanol Fuel Cells Catalyst Layers, J. Fuel Cell Sci. Technol. 10 (2013).
[22] A. Burdzik, M. Stähler, I. Friedrich, M. Carmo, D. Stolten, Homogeneity analysis of square meter-sized electrodes for PEM electrolysis and PEM fuel cells, J. Coat. Technol. Res. 15 (2018) 1423–1432.
[23] S.A. Mauger, K. Neyerlin, A.C. Yang-Neyerlin, K.L. More, M. Ulsh, Gravure Coating for Roll-to-Roll Manufacturing of Proton-Exchange-Membrane Fuel Cell Catalyst Layers, J. Electrochem. Soc. 165 (2018) F1012–F1018.
[24] S. Goswami, S. Klaus, J. Benziger, Wetting and Absorption of Water Drops on Nafion Films, Langmuir. 24 (2008) 8627–8633. https://doi.org/10.1021/la800799a.
[25] J. Geens, K. Peeters, B. Van der Bruggen, C. Vandecasteele, Polymeric nanofiltration of binary water–alcohol mixtures: influence of feed composition and membrane properties on permeability and rejection, J. Membr. Sci. 255 (2005) 255–264.
[26] S. Khandavalli, J.H. Park, N.N. Kariuki, S.F. Zaccarine, S. Pylypenko, D.J. Myers, M. Ulsh, S. Mauger, Investigation of the Microstructure and Rheology of Iridium Oxide Catalyst Inks for Low-Temperature Polymer Electrolyte Membrane Water Electrolyzers, ACS Appl. Mater. Interfaces. (2019).
[27] G. Bender, M. Carmo, T. Smolinka, A. Gago, N. Danilovic, M. Mueller, F. Ganci, A. Fallisch, P. Lettenmeier, K.A. Friedrich, K. Ayers, B. Pivovar, J. Mergel, D. Stolten, Initial approaches in benchmarking and round robin testing for proton exchange membrane water electrolyzers, Int. J. Hydrog. Energy. 44 (2019) 9174–9187. https://doi.org/10.1016/j.ijhydene.2019.02.074.

[28] H. Liu, C. Cai, M. Jia, J. Gao, H. Yin, H. Chen, Experimental investigation on spray cooling with low-alcohol additives, Appl. Therm. Eng. 146 (2019) 921–930.
[29] C. Reichardt, T. Welton, Solvents and solvent effects in organic chemistry, John Wiley & Sons, 2011.
[30] J. Elliott, S. Hanna, A. Elliott, G. Cooley, The swelling behaviour of perfluorinated ionomer membranes in ethanol/water mixtures, Polymer. 42 (2001) 2251–2253.
[31] T. Van Cleve, S. Khandavalli, A. Chowdhury, S. Medina, S. Pylypenko, M. Wang, K.L. More, N.N. Kariuki, D.J. Myers, A.Z. Weber, Dictating Pt-based Electrocatalyst Performance in Polymer Electrolyte Fuel Cells; from Formulation to Application, ACS Appl. Mater. Interfaces. (2019).
[32] A.S. Negi, C.O. Osuji, New insights on fumed colloidal rheology—shear thickening and vorticity-aligned structures in flocculating dispersions, Rheol. Acta. 48 (2008) 871–881. https://doi.org/10.1007/s00397-008-0341-9.
[33] L. Bergström, Shear thinning and shear thickening of concentrated ceramic suspensions, Colloids Surf. Physicochem. Eng. Asp. 133 (1998) 151–155.
[34] S. Khandavalli, J.H. Park, N.N. Kariuki, D.J. Myers, J.J. Stickel, K. Hurst, K.C. Neyerlin, M. Ulsh, S.A. Mauger, Rheological Investigation on the Microstructure of Fuel Cell Catalyst Inks, ACS Appl. Mater. Interfaces. 10 (2018) 43610–43622.
[35] J. Chinnam, D.K. Das, R.S. Vajjha, J.R. Satti, Measurements of the surface tension of nanofluids and development of a new correlation, Int. J. Therm. Sci. 98 (2015) 68–80.
[36] K.B. Singh, M.S. Tirumkudulu, Cracking in drying colloidal films., Phys. Rev. Lett. 98 (2007) 218302. https://doi.org/10.1103/PhysRevLett.98.218302.
[37] P. Trinke, G. Keeley, M. Carmo, B. Bensmann, R. Hanke-Rauschenbach, Elucidating the Effect of Mass Transport Resistances on Hydrogen Crossover and Cell Performance in PEM Water Electrolyzers by Varying the Cathode Ionomer Content, J. Electrochem. Soc. 166 (2019) F465–F471.
[38] S.M. Alia, H2@Scale: Experimental Characterization of Durability of Advanced Electrolyzer Concepts in Dynamic Loading, (2019). https://www.hydrogen.energy.gov/pdfs/review19/ta022_alia_2019_o.pdf.